A&A 496, 677–682 (2009)
DOI: 10.1051/0004-6361/200810365

Astronomy & Astrophysics

The molecular gas content of blue dwarf galaxies⋆

A collapsing detached molecular system in He 2–10?

L. Vanzi[1,2], F. Combes[3], M. Rubio[4], and D. Kunth[5]

[1] Departamento de Ingeniera Electrica, Pontificia Universidad Catolica de Chile, Av. Vicuña Mackenna 4860, Santiago, Chile
e-mail: lvanzi@ing.puc.cl
[2] European Southern Observatory, Alonso de Cordoba 3107, Vitacura, Santiago, Chile
[3] Observatoire de Paris, 61 Av. de l'Observatoire, 75014 Paris, France
[4] Departamento de Astronomia, Universidad de Chile, Casilla 36-D, Santiago, Chile
[5] Institut dAstrophysique de Paris, 98bis Bd Arago, 75014 Paris, France

Received 10 June 2008 / Accepted 20 January 2009

ABSTRACT

We present new observations of a sample of blue dwarf galaxies in the lines of CO(3–2) and HCN(4–3). The observations were obtained with the 12 m APEX telescope located at an altitude of 5100 m in Chajnantor (ALMA site). We detected CO(3–2) emission in seven of nine observed galaxies in our sample. In two galaxies, NGC 5253 and He 2–10, we mapped the central $20'' \times 20''$ in the CO(3–2) emission line. In He 2–10, we detected an extended component of molecular gas to the north-east of the main body of the galaxy. Comparing our data with previous HI and CO observations, we speculate that the presence of this detached cloud of molecular gas is produced by the merger already known in He 2–10, and could lead to the formation of a small tidal dwarf galaxy. The HCN(4–3) line was observed in NGC 5253 and He 2–10 only, but not detected.

Key words. galaxies: dwarf – galaxies: ISM – galaxies: starburst

1. Introduction

Nearby blue dwarf galaxies offer a laboratory to test the physical conditions of star formation in the early universe. Star formation in giant galaxies must have occurred differently at high redshift when the content of heavy elements, molecular gas and dust was much lower than today. Although molecular gas and dust have been detected at high redshift (Ledoux et al. 2003; Sheth et al. 2004; Bertoldi et al. 2003), the modes through which they were produced are not clear, as we still do not have the details of how star formation could have proceeded at that epoch from a pristine ISM. Beyond $z = 6$, when the Universe was younger than 1 Gyr, supernovae seem to offer the only efficient way for dust production (Maiolino et al. 2004). Blue dwarf galaxies resemble the conditions that we expect must have characterized the early Universe. They are experiencing intense starbursts, as revealed by their blue optical colors and spectra. Their metal content is typically lower than solar and among them the least chemically evolved galaxies in the Universe are found. Other evidence that make them good laboratories for the study of early star formation includes the very high fractional neutral hydrogen gas content (Thuan & Martin 1981) and the lack, or the weak presence, of an evident underlying old stellar population in optical and near-infrared images. For these reasons, ever since their discovery as a class of objects in the early 70s, blue dwarf galaxies even have been thought of as excellent candidates for being young galaxies, i.e. systems presently undergoing one of their very first bursts of star formation (Searle & Sargent 1972). Such a possibility though has now been excluded in most cases (e.g. Kunth & Östlin 2000; Aloisi et al. 2007).

In most galaxies, the CO molecule can be easily detected through its emission lines in the millimetre spectral region, and is the best tracer of molecular gas, since H_2 does not radiate in its coldest phases. However, dwarf galaxies do not show CO emission, most of them in fact are not detected or detected at a very low level (e.g. Taylor et al. 1998; Gondhalekar et al. 1998; Leroy et al. 2005) and they are generally thought of as being devoid of dust, due to the lack of heavy elements. The lack of observed CO is then attributed to an exceptionally low CO/H_2 ratio (Arnault et al. 1988; Taylor et al. 1998) rather than to an intrinsic lack of molecular hydrogen.

The HCN molecule has been detected in a number of starburst and ultraluminous IR galaxies (Gao & Solomon 2004) but so far only in very few dwarfs as the Magellanic Clouds (Chin et al. 1997, 1998) and in the peculiar starburst dwarf M 82 (Sorai et al. 2002). The HCN(4–3) line is a tracer of density, and its relative strength with respect to the CO line is a tracer of starburst activity (Gao & Solomon 2004). HCN emission is strongly correlated to the infrared luminosity, indicating that starbursts are very intense in dense molecular clouds. Towards the center of AGN galaxies, the HCN/CO ratio is also enhanced, due to the activity of the nucleus, in particular the X-ray excitation (Kohno et al. 2003), but this involves a small central region, and would be visible for only very nearby objects, where the spatial resolution is sufficient.

We took advantage of the unique atmospheric conditions offered by the Chajnantor plane, the future ALMA site, to observe a sample of blue dwarf galaxies with APEX in the CO(3–2) and HCN(4–3) lines. This was mostly a pilot project, to assess

⋆ Based on observations obtained at APEX under program 077.B-0307.

Table 1. Main properties of the sample galaxies and CO line detections (K km s^{-1}) derived from the literature.

Name	D (Mpc)	12 + Log(O/H)	CO(1, 0)	CO(2, 1)	CO(3, 2)
He 2–10	9[K9]	8.93[K9]	10.0 (40″)[Ba], 4.85(55″)[K5]	17.3 (21″)[Ba], 6.82 (27″)[K5]	36.8 (14.″5)[Ba], 16.6 (22″)[Me]
IC 745	16.3[1], 15.4[Tu]	8.9[Sa]	1.12 (22″)[Sa]	1.02 (12.″5)[Sa]	–
NGC 4123	22.4[We], 25.3[Tu]	9.05[Ra]	4.5 (35″)[Go], 17.8 (22″)[Kr]	32.7 (12″)[Kr]	
NGC 4309	18.0[Fo]		3.01 (55″)[Le]		–
NGC 4385	33.5[Tu]	9.1[Ma]	6.2 (35″)[Go], 6.8 (15″)[De], 2.3 (44″)[Tc]		5.0 (14″)[De]
NGC 4630	17.9[Tu], 20[Al]		4.45 (55″)[Le], 3.86 (24″)[Al]	4.84 (11″)[Al]	
NGC 4701	20.5[Tu]		4.85 (55″)[Le], 2.90 (21″)[Bo]	3.02 (11″)[Bo]	
NGC 4713	17.9[Tu]	8.84[Sk]	3.61(55″)[Le]		
NGC 5253	3.3[Fe]	8.14[K9]	0.72 (55″)[Ty], 1.3 (44″)[Wi]		3.39 (22″)[Me]

(1) Distance assuming H_0 = 70 km s^{-1} Mpc^{-1}; (Al) Albrecht et al. (2004) – IRAM 30 m; (Ba) Baas et al. (1994) – SEST 15 m; (Bo) Boker et al. (2003) – IRAM 30 m; (De) Devereux et al. (1994) – NRO 45 m; (Fe) Ferrarese et al. (2000); (Fo) Fouque et al. (2001); (Go) Gondhalekar et al. (1998) – OSO 20 m; (K5) Kobulnicky et al. (1995) – NRAO 12 m; (K9) Kobulnicky et al. (1999); (Kr) Krugel et al. (1990) – IRAM 30 m; (Le) Leroy et al. (2005) – NRAO 12 m; (Ma) Mayya et al. (2004); (Me) Meier et al. (2001) – CSO 10.4 m; (Ra) Raimann et al. (2000); (Sa) Sage et al. (1992) – IRAM 30 m; (Sk) Skillman et al. (1996); (Tu) Tully (1988); (Tc) Tacconi et al. (1991) – SEST 15 m; (Ty) Taylor et al. (1998) – NRAO 12 m; (We) Weiner et al. (2001); (Wi) Wiklind & Henkel (1989) – SEST 15 m.

the new instrument capabilities, and prepare more challenging projects.

This paper is organized as follow: in Sect. 2 we briefly describe the observations, in Sect. 3 we present the analysis of the data including line profiles, deriving column densities and excitation. Section 4 describes the peculiar case of He 2–10, in which extended CO emission has been found, and in Sect. 5 we summarize our conclusions.

2. Observations

The sample galaxies were selected from the works of Sage et al. (1992), Taylor et al. (1998), Gondhalekar et al. (1998), Israel (2005), Leroy et al. (2005), to have firm detections of the CO(1–0) or CO(2–1) lines. They also span a luminosity range, hence a metallicity range, from sub solar to nearly solar. In some cases metallicities have been directly measured from their HII regions (i.e. NGC 5253). The sample galaxies and their main properties are listed in Table 1.

The observations were obtained during the ESO period 77, spanning from April to September 2006, with the Apex-2a receiver mounted at one of the Nasmyth foci of the APEX antenna. The Atacama Pathfinder EXperiment (APEX) is located at an altitude of 5100 m in Chajnantor, close to the future site of ALMA; the antenna has a diameter of 12 m. The Apex-2a is a heterodyne receiver covering the band 279–381 GHz. The backend is provided by a Fast Fourier Transform Spectrometer (FFTS) with a 1 GHz band and 8192 channels. The system temperature ranged from 270 to 800 K. The pointing accuracy is better than 5″. We observed in the lines of CO(3–2) at 345.796 GHz and HCN(4–3) at 354.506 GHz. The APEX beam at these frequencies is about 19–20″. For NGC 5253 and He 2–10 we also obtained a 3 × 3 map with offsets of 20″ in RA and Dec. For the telescope pointing we used the coordinates listed by the NASA/Ipac Extragalactic Database (NED) for the 2000 equinox.

The data were reduced with CLASS[1] following a standard procedure. First order polynomials were used for baseline subtraction. The spectra were smoothed to a velocity resolution of 4.2 km s^{-1}. The CO(3–2) line was detected in 7 out of 9 galaxies. Only He 2–10 and NGC 5253 were observed in the HCN(4–3) line; neither galaxy was detected. For the lines detected we ran a Gaussian fit to determine the line intensity. Antenna temperatures were converted to main beam temperatures by using a beam efficiency of 0.70. CO(3–2) spectra of the central position of five galaxies are shown in Fig. 1. The CO(3–2) map of NGC 5253 and He 2–10 are shown in Figs. 2 and 3. The line intensities, velocities and velocity dispersions obtained from Gaussian fits for our sample are shown in Table 2. The 1σ level of the spectra with no detection was 0.016 K.

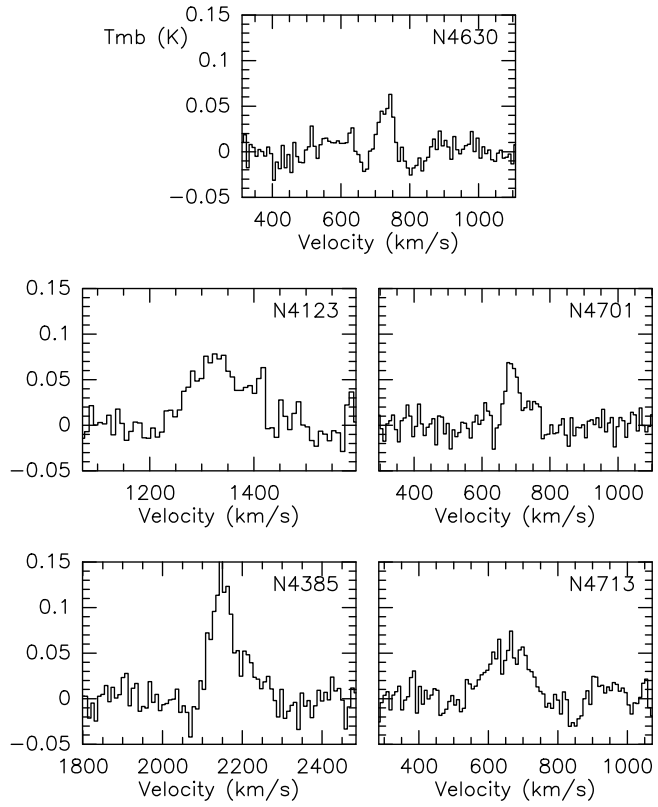

Fig. 1. CO(3–2) spectra of five galaxies detected in the observed sample. The spectra have been smoothed to 8.4 km s^{-1} in velocity.

3. Analysis of the seven dwarfs detected

In this section we derive the physical parameters of the molecular gas, combining our observations with the previous CO lines detected in the literature.

[1] http://www.iram.fr/IRAMFR/GILDAS

Table 2. CO(3–2) intensities, velocities, and velocity dispersions from Gaussian fits to the central positon of the sample of galaxies observed. Errors derived from the Gaussian fits are indicated in parenthesis. The detections at two positions are indicated for He 2–10, at the offset position (20, 20) the parameters for the two lines detected are reported.

Source	T_{mb} (mK)	V_{lsr} (km s^{-1})	DV (km s^{-1})	Ico (K km s^{-1})
NGC 4123	68.	1333. (5)	124. (10)	9.0 (0.6)
NGC 4385	124.	2151. (2)	66. (5)	8.7 (0.6)
NGC 4630	54.	732. (3)	42. (5)	2.4 (0.3)
NGC 4701	66.	689. (3)	46. (7)	3.2 (0.4)
NGC 4713	54.	656. (5)	127. (10)	7.3 (0.6)
NGC 5253	82.	401. (1)	36. (2)	3.1 (0.1)
He2–10				
(0, 0)	312.	850. (0.4)	53. (1.)	17.6 (0.3)
(20, 20)	130.	787. (1.7)	52. (4.)	7.2 (0.5)
(20, 20)	113.	933. (1.2)	17. (2.)	2.0 (0.3)
IC 745	–	–	–	–
NGC 4309	–	–	–	–

The CO(3–2) emission in all galaxies observed is very weak, $T_{mb} \approx 0.05$ K, consistent with previous observations towards dwarf starburst galaxies (Meier et al. 2001) and irregular ones (Young et al. 1984; Sage et al. 1992; Young and Scoville 1982, and references therein). Observations in the CO lines of the observed sample obtained from the literature are listed in Table 1.

3.1. Line ratios

Except for He 2–10 and NGC 5253, which have been mapped, the distances of the detected dwarfs are greater than 18 Mpc. The size of our CO(3–2) beam is then larger than 1.7 kpc on the galaxy, which means that the emission is expected to be point-like in CO. It is therefore with the point source approximation that we determined CO(3–2)/CO(1–0) and CO(3–2)/CO(2–1) ratios for the galaxies where information on CO(2–1) and CO(1–0) emission line was available. We thus applied beam ratios for the different telescopes used to make this comparison.

The results are shown in Table 3 for all the galaxies which were observed in one position. The CO(3–2)/CO(1–0) ratios range between 0.22 in NGC 4713 to 0.82 in NGC 4701. We determine the CO(3–2)/CO(2–1) ratios only for four of our galaxies. These ratios are in a similar range as those obtained by Meier et al. (2001).

In the case of NGC 4385, NGC 4630, NGC 4701, CO(1–0) observations with more than one telescope were available. We used the emission obtained from the smallest beam size telescope for our comparison, when the total integrated emission was similar when observed with a larger and a smaller beam, an indication that the source was indeed unresolved and that the observations with larger beam size telescopes suffered from beam filling factors. As an example, for NGC 4385 the total integrated emission in CO(1–0) for a 35″ beam and 15″ is 6.2 K km s^{-1} and 6.8 K km s^{-1} respectively. Thus we have assumed that the size of this source is ∼15″.

In He 2–10, we obtain at the center position a CO(3–2)/CO(1–0) line ratio of about 0.4 when compared to two independent CO(1–0) observations and a CO(3–2)/CO(2–1) of 0.7. These ratios are consistent with optically thick molecular gas, but with a temperature lower than 50 K, or a high kinetic temperature, but a sub-thermal excitation, due to an average gas density lower than $n(H_2) = 10^4$ cm^{-3} (see Bayet et al. 2004).

Table 3. CO line ratios, computed with the approximation of unresolved sources. In the case of He 2–10 and NGC 5253 the ratios were computed using two different CO(1–0) observations reported in the literature.

Source	CO(3–2)/CO(1–0)	CO(3–2)/CO(2–1)
He 2–10 (0, 0)	0.36	0.74
	0.39	0.71
NGC 4123	0.52	0.62
NGC 4309	–	–
NGC 4385	0.37	–
	0.66	–
NGC 4630	0.35	1.35
NGC 4701	0.82	2.87
NGC 4713	0.22	–
NGC 5253	0.46	–
	0.39	–

3.2. Spatial distribution

For NGC 5253 and He 2–10 we observed a map in CO(3–2). These two galaxies have also been observed with the 14 m Caltech submillimeter telescope (CSO) (Meier et al. 2001). Our observations are consistent with those, in particular no extended emission was observed in NGC 5253, while we detected extended CO(3–2) emission in the map of He 2–10. For the positions previously observed by other researchers (Meier et al. 2001; Baas et al. 1994) our observations give consistent intensities after convolving to a similar resolution. However we also detected CO at locations not observed before, in particular to the NE of the galaxy. At our position (20″, 20″) we observed for the first time two well separated velocity components at 787.6 km s^{-1} and 933 km s^{-1}. Meier et al. (2001) at their NE position (10″, 20″) detected a component at a velocity of 826 km s^{-1}; our data show weak emission at this position at a similar velocity. This component is shifted by about 25 km s^{-1} with respect to the CO detected in the central position of the galaxy which is centered at 850 K m/s, also detected by Meier et al. (2001) and Baas et al. (1994). We have determined line ratios for the central velocity component assuming that the same emission detected by Meier et al. (2001) is seen in our 20″ beam.

The component detected in CO(3–2) at 933 km s^{-1} was not reported earlier. The integrated flux is low but well detected with an intensity Ico = 2.1 ± 0.3 K km s^{-1}; the line is narrower compared to the component at 780 km s^{-1}.

This new component has a high CO(3–2)/CO(1–0) ratio and thus could be a warm and dense detached molecular cloud from the merger.

4. The peculiar case of He 2–10

4.1. The merging state of He 2–10

Henize 2–10 is a nearby blue dwarf galaxy (D = 9 Mpc) which hosts an intense episode of star formation as revealed by clasical indicators such as the strong optical and infrared emission lines (Vacca & Conti 1992; Vanzi & Rieke 1997), the detection of Wolf-Rayet features (Vacca & Conti 1992), intense mid-IR (Sauvage et al. 1997) and far-IR continuum (Johansson 1987).

Due to its relatively close distance and quite remarkable properties, He 2–10 has been studied in detail in the past and it has provided relevant insights into the starburst phenomenon. Johnson et al. (2000) observed He 2–10 with the WFPC2 on board the HST and detected a number of young super massive clusters in the star forming region of the galaxy with typical

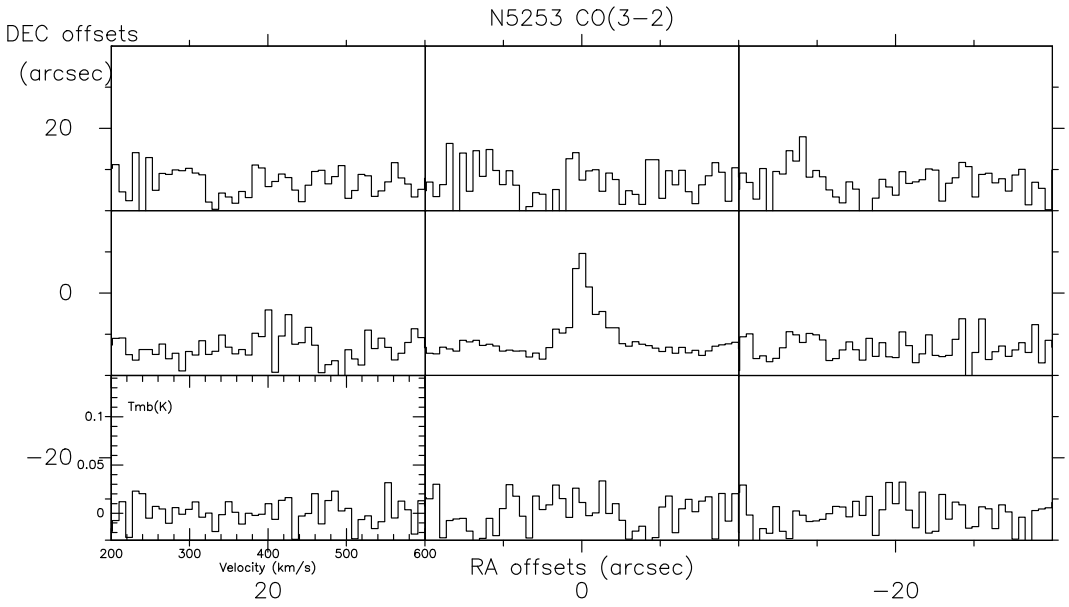

Fig. 2. CO(3–2) map of NGC 5253. Nine positions spaced every 20 arcsec were observed. The spectra have been smoothed to 8.4 km s^{-1}. Emission is detected in the center position (0, 0) only.

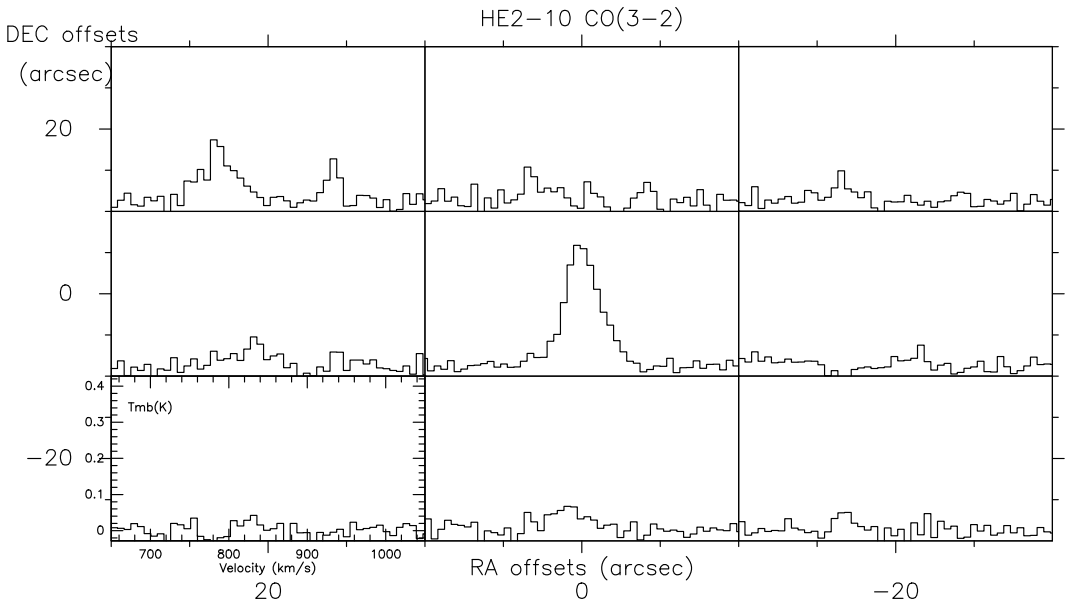

Fig. 3. CO(3–2) map of He 2–10. Nine positions spaced every 20 arcsec were obsserved. The spectra have been smoothed to 8.4 km s^{-1}. Emission is detected in the center position (0, 0) at 850.6 km s^{-1}, in the NE at (+20″, +20″) offset at 787.6 km s^{-1} and 933.1 km s^{-1}. These velocity components are weakly detected in 2 or 3 other positions.

masses up to 10^5 $M_\odot$ and ages of few Myr. Some compact radio sources were observed by Johnson & Kobulnicky (2003) who characterized their spectra as thermal, measured their sizes as 2–4 pc and their masses in excess of 10^5 $M_\odot$. Cabanac et al. (2005) observed in the IR and detected several compact sources that could be associated with the radio sources previously mentioned; they interpreted most of them as ultracompact HII regions and two as possible SN remnants.

Observations of CO(1–0), CO(2–1) (single dish NRAO 12 m and Owens Valley Interferometer) and HI 21cm (VLA) were obtained by Kobulnicky et al. (1995), they derived a total molecular gas mass of 1.6×10^8 $M_\odot$ and an atomic gas mass of 1.9×10^8 $M_\odot$. Thanks to the interferometric resolution, they detected, besides the central concentration, a CO plume extended about 30″ to the south east; a similar but more extended feature is detected in HI. They interpreted these features as a sign of a merger. CO(3–2) is detected by Meier et al. (2001) with the CSO 10.4 m single dish. They could only partially confirm the SE extension observed by Kobulnicky et al. (2005).

4.2. Detection of two velocity components

As plotted in Fig. 3 the CO(3–2) map is extended, and suprisingly we clearly detect CO at two velocities, 787 and 933.1 km s^{-1} at the position (20″, 20″). Much weaker lines at 787, 850 and 933 km s^{-1} are detected to the north of the galaxy center, at our position (0, 20). The parameters of these detections are given in Table 2. At position (–20, 20), we see a hint of emission at these two velocity components but no hint of the 850 km s^{-1} emission. Similarly to Meier et al. (2001) we do not

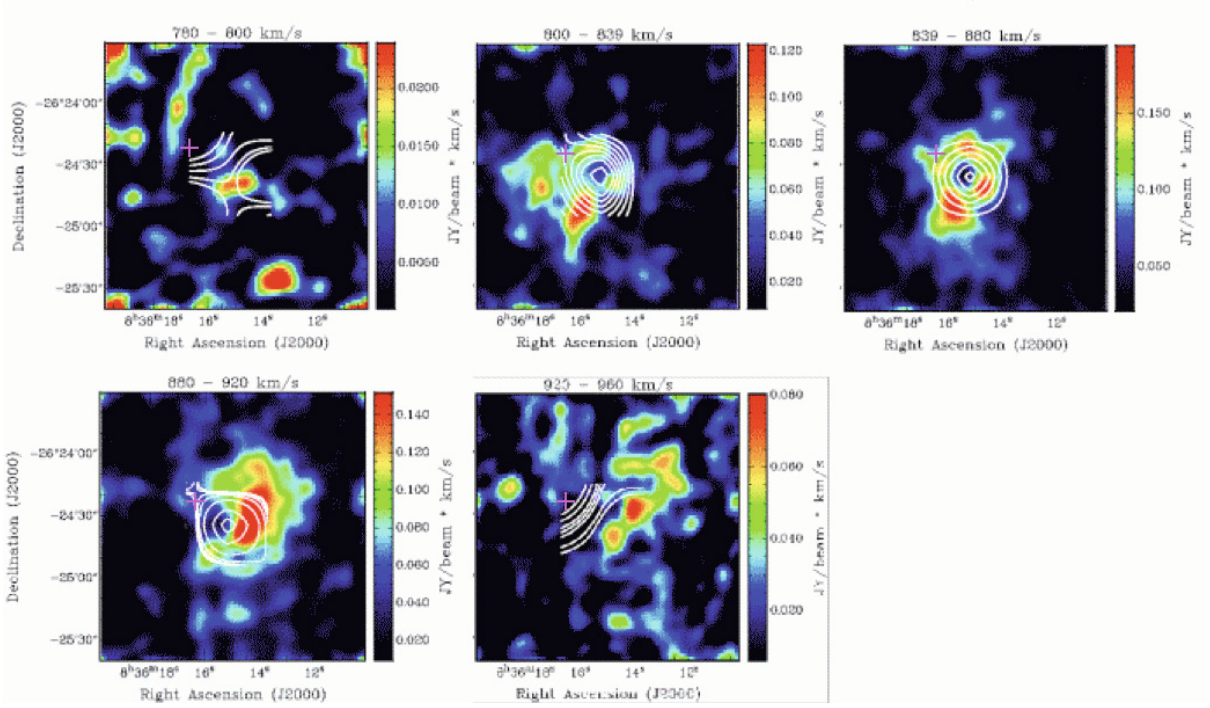

Fig. 4. Comparison of the HI observations of Kobulnicky et al. (1995) in color scale and our own CO(3–2) contours superimposed. The molecular gas of the galaxy as traced by the CO emission shows a spatially centered distribution. The CO gas changes its spatial distribution at the highest velocity range (920–960) and a new NE component is begining to be seen. In the HI map a NE component at the same velocity is seen. The feature detected by Kobulnicky et al. (1995) is at offset (17″, 10″). Because of the few points observed the contours of the CO(3–2) have been selected to optimize the visibility of the features; they are as follows in the panels: 780–800 km s^{-1} (0.1 0.25 0.5 1 1.6 2.2 K km s^{-1}), 800–839 km s^{-1} (0.5 1 1.5 2 2.5 3 3.5 4 4.8 K km s^{-1}), 839–880 km s^{-1} (0.4 2 4 6 8 10 12 K km s^{-1}), 882–924 km s^{-1} (0.1 0.15 0.2 0.3 0.5 1 2 2.8 K km s^{-1}), 920–960 km s^{-1} (0.1 0.2 0.4 0.5 0.6 0.8 1 K km s^{-1}).

see any evidence of the extended emission toward the south-east denoted as C by Kobulnicky et al. (1995). Our detection to the north-east of the galaxy at the position (20, 20) finds support in the feature denoted as D by Meier et al. (2001) but with slightly different velocities.

One of the velocity features present in the north-east position is expected from the rotation curve, and comes from the normal disk of the galaxy: this is the lower velocity component, at 787 km s^{-1}. The higher velocity component, at 933 km s^{-1}, is actually a detached feature, which must come from the tidal interaction experienced by the galaxy. At this position, there is a tidal tail already detected in HI by Kobulnicky et al. (1995). A weak emission of this velocity component is also seen at (0, 20), a Gaussian fit of this component gives a center velocity of 933 km s^{-1}, a linewidth of 15 km s^{-1} and an intensity of 0.55 ± 0.02 K km s^{-1}, about three times less than the value obtained in the Gaussian fit in the spectrum towards (20, 20). A hint of emission at this same velocity is suggested at (20, 0). From these values, and assuming an optically thick medium, warm and not sub-thermally excited, we deduce a molecular mass of $1.4 \times 10^7\ M_\odot$, assuming a standard CO to H_2 conversion ratio of 2.3×10^{20} cm^{-2}/(K km s^{-1}) (e.g. Strong et al. 1988).

We have compared our CO observations with those of neutral hydrogen, HI, of Kobulnicky et al. (1995). In Fig. 4 our CO contours are overlayed on the color scale HI maps in 5 velocity beams. The central CO condensation at a velocity of 850 km s^{-1} denotes the gravitational center of He 2–10. The HI map shows a ring structure around the CO center which is typical of dense regions where the gas becomes molecular.

We find that there is weak HI emission in the velocity contour map (920–960 km s^{-1}) where the CO emission begins to be strong. This new feature can be considered as a detached cloud expelled in the merger, which He 2–10 is experiencing. We propose an interpretation of this feature as a dense and hot gas cloud collapsing in a tidal tail to form a possible star forming region, although no star cluster is yet found at this position, as can be seen on the V-image from Kobulnicky et al. (1995) and in the Ks image of Vanzi & Sauvage (2006). The HST image does not extend as far as this position, unfortunately.

4.3. Why the NE detached component was not discovered before

Kobulnicky et al. (1995) carried out an interferometer CO(1–0) study with OVRO of He 2–10, with a synthezised beam of 6.5″ × 5.5″. They found a remarkable CO tidal tail towards the south-east; their map also reveals the hint of a CO(1–0) detached clump emission towards the north-east, at high velocity, although they do not comment on that, interpreting this feature as noise. Here we see for the first time a strong signal in the north-east, which could be due to a clump in a tidal tail, similar to those collapsing in tidal dwarf galaxies. (see e.g. simulations by Duc et al. 2004). Obviously this NE clump is highly excited, emitting much stronger in CO(3–2) than in CO(1–0). Baas et al. (1994) do not see this clump, since their map does not extend into this region (their beam with the JCMT is smaller than ours). Meier et al. (2001) have also observed in CO(3–2) with the CSO (beam of 22″) and made a small map, with a sampling of 10″. However, their map was not extended enough to reach the (20, 20) point; in consequence, the contours in their Fig. 7 suggest a CO(3–2) extension to the NE, but they do not detect it entirely. They confirm though that the south-east tidal tail, very prominent in

CO(1–0), is not obvious in CO(3–2), implying a quite cold component. They confirm the existence of a detached feature also, at position (18″, 9.5″) relative to the center. The actual position of the maximum might be underestimated in declination, due to the truncation of their map.

When compared to the HI map obtained with the VLA by Kobulnicky et al. (1995), we notice that the CO detached component in the NE has an HI counterpart, in a tidal tail. This supports the hypothesis of a giant clump of gas collapsing in a tidal tail to form a small tidal dwarf galaxy.

5. Conclusions

We observed a sample of starbursting dwarf galaxies in the lines CO(3–2) and HCN(4–3) at 350 GHz with the Apex-2a heterodyne receiver attached to the APEX telescope at the Chajnantor site, in Chile. These dwarf galaxies were already detected in lower J CO lines in the literature. We compared the CO(3–2) results with previous data and determined the molecular gas excitation state. Most galaxies are detected in CO(3–2), with low line ratios, suggesting optically thick emission with moderate temperature and/or moderate density. In a few regions, however, the line ratio is high, implying a hot and dense star forming locations. No HCN(4–3) line was detected, at a sensitivity of 5 mK.

The most interesting observation was towards the blue dwarf galaxy He 2–10, that was mapped in the CO(3–2) and found extended. The main conclusions are:

1. CO(3–2) emission was detected in a $20'' \times 20''$ area at a sensitivity of 18 mK. We detected for the first time CO emission at a second velocity of 933 km s^{-1} at position $(20, 20)$. At position $(0, 20)$ there is also a weak hint of emission in this velocity.
2. The 933 km s^{-1} CO velocity component is detected at the same position in the galaxy where weak HI emission had been detected. This component is interpreted as evidence of a detached cloud expelled in the merger that He 2–10 is experiencing.
3. The detached cloud has a mass of about $1.4 \times 10^7\ M_\odot$, with no stars in it yet. However the high CO(3–2)/CO(1–0) line ratios suggests a hot and dense molecular gas, which could be collapsing towards the formation of new star cluster, as it is frequently observed in tidal dwarf galaxies.

Acknowledgements. We are happy to thank Chip Kobulnicky for giving his HI data cube on He 2–10 in order to make the comparison of Fig. 4. This research has made use of the NASA/IPAC Extragalactic Database (NED) which is operated by the Jet Propulsion Laboratory, California Institute of Technology, under contract with the National Aeronautics and Space Administration. We also used the CLASS software that was developed at the Observatoire de Grenoble and IRAM. M.R. is supported by the Chilean *Center for Astrophysics* FONDAP No. 15010003.

References

Albrecht, M., Chini, R., Krügel, E., et al. 2004, A&A, 414, 141
Aloisi, A., Clementini, G., Tosi, M., et al. 2007, ApJ, 667, L151
Arnault, P., Kunth, D., Casoli, F., & Combes, F. 1988, A&A, 205, 41
Baas, F., Israel, F. P., & Koornneef, J. 1994, A&A, 284, 403
Bayet, E., Gerin, M., Phillips, T. G., & Contursi, A. 2004, A&A, 427, 45
Bertoldi, F., Cox, P., Neri, R., et al. 2003, A&A, 409, L47
Böker, T., Lisenfeld, U., & Schinnerer, E. 2004, A&A, 406, 87
Cabanac, R., Vanzi, L., & Sauvage, M. 2005, ApJ, 631, 252
Chin, Y. N., Henkel, C., Whiteoak, J. B., et al. 1997, A&A, 317, 548
Chin, Y. N., Henkel, C., Millar, T. J., et al. 1998, A&A, 330, 901
Devereux, N., Taniguchi, Y., Sanders, D. B., et al. 1994, AJ, 107, 2006
Duc, P.-A., Bournaud, F., & Masset, F. 2004, A&A, 427, 803
Ferrarese, L., Mould, J. R., Kennicutt, R. C. Jr., et al. 2000, ApJ, 529, 745
Fouqué, P., Solanes, J. M., Sanchis, T., & Balkowski C. 2001, A&A, 375, 770
Galliano, F., Madden, S. C., Jones, A. P., Wilson, C. D., & Bernard, J.-P. 2005, A&A, 434, 867
Gao, Y., & Solomon, P. M. 2004, ApJS, 152, 63
Gerin, M., & Phillips, T. G. 2000, ApJ, 537, 644
Gondhalekar, P. M., Johansson, L. E. B., Brosch, N., et al. 1998, A&A, 335, 152
Henry, A. L., Turner, J. L., Beck, S. C., et al. 2007, AJ, 133, 757
Israel, F. P. 2005, A&A, 438, 855
Johansson, I. 1987, A&A, 182, 179
Johnson, K. E., & Kobulnicky, H. A. 2003, ApJ, 597, 923
Johnson, K. E., Leitherer, C., Vacca, W. D., & Conti, P. S. 2000, AJ, 120, 1273
Kobulnicky, H. A., Dickey, J. M., Sargent, A. I., Hogg, D. E., & Conti, P. S. 1995, AJ, 110, 116
Kobulnicky, H. A., Kennicutt, R. C. Jr., & Pizagno, J. L. 1999, ApJ, 514, 544
Kohno, K., Ishizuki, S., Matsushita, S., et al. 2003, PASJ, 55, L1
Krügel, E., Steppe, H., & Chini, R. 1990, A&A, 229, 17
Kunth, D., & Ostlin, G. 2000, A&AR, 10, 1
Ledoux, C., Petitjean, P., & Srianand, R. 2003, MNRAS, 346, 209
Leroy, A., Bolatto, A. D., Simon, J. D., & Blitz, L. 2005, ApJ, 625, 763
Maiolino, R., Schneider, R., Oliva, E., et al. 2004, Nature, 431, 533
Mayya, Y. D., Bressan, A., Rodriguez, M., et al. 2004, ApJ, 600, 188
Martin-Hernandez, N. L., Schaerer, D., Peeters, E., Tielens, A. G. G. M., & Sauvage, M. 2006, A&A, 455, 853
Meier, D. S., Turner, J. L., Crosthwaite, L. P., & Beck, S. C. 2001, AJ, 121, 740
Raimann, D., Storchi-Bergmann, T., Bica, E., et al. 2000, MNRAS, 316, 559
Sage, L. J., Salzer, J. J., Loose, H. H., & Henkel, C. 1992, A&A, 265, 19
Sauvage, M., Thuan, T. X., & Lagage, P. O. 1997, A&A, 325, 98
Searle, L., & Sargent W. L. W. 1972, ApJ, 173, 25
Sorai, K., Nakai, N., Kuno N., & Nishiyama K. 2002, PASJ, 54, 179
Sheth, K., Blain, A. W., Kneib, J. P., et al. 2004, ApJ, 614, L5
Skillman, E. D., Kennicutt, R. C., Shields, G. A., & Zaritsky, D. 1996, ApJ, 462, 147
Strong, A. W., Bloemen, J. B. G. M., Dame, T. M., et al. 1988, A&A, 207, 1
Tacconi, L. J., Tacconi-Garman, L. E., Thornley, M., & van Woerden, H. 1991, A&A, 252, 541
Taylor, C. L., Kobulnicky, H. A., & Skillman, E. D. 1998, AJ, 116, 2746
Thuan, T. X., & Martin, G. E. 1981, ApJ, 247, 823
Tully, R. B. 1988, Nearby Galaxies Catalog (Cambridge University Press)
Vacca, W. D., & Conti, P. S. 1992, ApJ, 401, 543
Vanzi, L., & Rieke, G. H. 1997, ApJ, 479, 694
Vanzi, L., & Sauvage, M. 2006, A&A, 448, 471
Weiner, B. J., Williams, T. B., van Gorkm, J. H., & Sellwood, J. A. 2001, ApJ, 546, 916
Wiklind, T., & Henkel, C. 1989, A&A, 225, 1
Young, J. S., & Scoville, N. 1982, ApJ, 260, L11
Young, J. S., Gallagher J. S., & Hunter, D. A. 1984, ApJ, 276, 476